Proceedings of the 6th Nordic Signal Processing Symposium - NORSIG 2004
June 9 - 11, 2004
Espoo, Finland

Interference Suppression in MIMO HSDPA Communication

Jari Ylioinas, Kari Hooli, Kai Kiiskilä, Markku Juntti

Centre for Wireless Communications (CWC),
Tutkijantie 2E, P.O. Box 4500, FIN-90014, University of Oulu, Finland
e-mail: jari.ylioinas@ee.oulu.fi

ABSTRACT

Multiple transmit and receive antennas with spatial multiplexing are planned for wideband code division multiple access (WCDMA) systems. Thus, multiple–access interference (MAI) and inter–antenna interference (IAI) have to be mitigated. In this paper, a new linear receiver applicable for downlink employing long scrambling code is presented and compared to the known ones. These receivers equalize the channel and, thus, suppress MAI. Also IAI is mitigated by equalizing over the receive antennas. The proposed receiver is shown to provide a good performance–complexity trade–off for practical WCDMA terminal receivers.

1. INTRODUCTION

High speed downlink packet access (HSDPA) for wideband code division multiple access (WCDMA) is under development to enhance the downlink data rates beyond 10 Mbps. The use of multiple transmit and receive antennas, i.e., a multiple–input multiple–output (MIMO) channel provides potential for a tremendous capacity increase [1]. Spatial multiplexing, i.e., independent data stream transmission from different antennas, is available also for HSDPA [2] resulting in inter–antenna interference (IAI) [3].

Multipath propagation in a synchronous CDMA downlink causes also multiple–access interference (MAI), which can be mitigated efficiently by channel equalizers that retain the orthogonality of the spreading sequences to some extent [4, 5] also in the systems using long scrambling codes. Their simplest and the most practical versions approximate the interfering users' spreading sequences as random ones on chip level [4]. The channel equalizers are less effective to combat IAI than MAI, since different spatial channels apply the same spreading code.

In this paper, the linear minimum mean square error (LMMSE) channel equalizer and its two approximations are considered as terminal receivers for MIMO WCDMA HSDPA downlink to offer reasonable MAI and IAI mitigation with acceptable complexity. An improved LMMSE approximation is proposed based on despread correlator outputs, and its performance is compared to the already known approximation. To further enhance IAI mitigation, also optimum maximum *a posteriori* (MAP) detector in the space domain is considered as a benchmark and a concatenation of the LMMSE equalizer to mitigate residual MAI.

The research described in this paper has been supported by Nokia Mobile Phones and Texas Instruments what is gratefully acknowledged.

2. SYSTEM MODEL

The information bits of the desired user are protected with the rate 1/3 turbo code [6, 7]. The code is built as a parallel concatenation of two binary recursive systematic convolutional codes. Turbo encoder contains internal interleaver preceding the other constituent encoder, and the encoder is followed by a channel interleaver. The interleaving depth is the transmission time intervel (TTI), i.e., 2 ms [2]. The encoded bits are mapped into quadrature phase shift keying (QPSK) symbols on a single physical channel. Symbol stream on a physical channel is converted into parallel streams transmitted from N_{T} antennas with the same channelization and scrambling sequence.

After down-conversion, low-pass filtering, and sampling, the discrete-time signals from multiple receive antennas are interleaved into a single vector $\boldsymbol{r}$ defined as [4]

$$\boldsymbol{r} = \sum_{k=1}^{\mathcal{K}} \boldsymbol{DCS}_k \boldsymbol{A}_k \boldsymbol{b}_k + \boldsymbol{\eta} \in \mathbb{C}^{N_c N_s}, \tag{1}$$

where $\mathcal{K}$ is the number of transmitted physical channels, $\boldsymbol{D}$ is chip waveform matrix, $\boldsymbol{C}$ is channel coefficient matrix with L paths per transmit-receive antenna pair, $\boldsymbol{S}_k$ is spreading sequence matrix, $\boldsymbol{A}_k$ is amplitude matrix, $\boldsymbol{b}_k$ is symbol vector, and $\boldsymbol{\eta}$ is noise vector. The number of samples per chip is denoted with N_{s}, and it is product of the number of receive antennas N_{R} and samples per chip on each of the receive antenna branches. N_{c} denotes the length of observation window in chip intervals. Additional $N_{\mathrm{c,e}}$ chips are included to model the tails of symbols transmitted before and after the observation window.

Matrix $\boldsymbol{D}$ introduces the effects of the transmitted chip waveforms, receiver front-end filtering and delays for propagation paths. Multiplication with matrix $\boldsymbol{D}$ interleaves the signal samples from multiple antennas into one vector. The interleaving is realized by the Kronecker product, i.e., $\boldsymbol{D} = \mathcal{D} \otimes \mathbf{I}_{N_{\mathrm{R}}}$, where $\mathcal{D} \in \mathbb{R}^{N_c N_s / N_{\mathrm{R}} \times N_{\mathrm{R}} L (N_c + N_{c,e})}$ is a matrix with column vectors containing samples from properly delayed waveform of the nth chip for the lth path. Matrix

$$\boldsymbol{C} = [\boldsymbol{C}_1, ..., \boldsymbol{C}_{N_{\mathrm{T}}}] \in \mathbb{C}^{N_{\mathrm{R}} L (N_c + N_{c,e}) \times N_{\mathrm{T}} (N_c + N_{c,e})} \tag{2}$$

contains channel coefficients in block diagonal matrices $\boldsymbol{C}_{n_{\mathrm{T}}} \in \mathbb{C}^{N_{\mathrm{R}} L (N_c + N_{c,e}) \times (N_c + N_{c,e})}$, in which column vectors contain the time-variant channel coefficients for L paths of N_{R} antennas. Block diagonal spreading sequence matrix

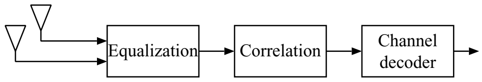

Fig. 1. Block-diagram of a receiver with equalization.

$\boldsymbol{S}_k$ is defined as $\boldsymbol{S}_k = \mathbf{I}_{N_\mathrm{T}} \otimes \boldsymbol{S}_{k,\mathrm{T}}$ where the block diagonal matrix $\boldsymbol{S}_{k,\mathrm{T}} \in \Xi_\mathrm{C}^{(N_c+N_{c,e})\times M_k}$ (Ξ_C is chip alphabet) contains spreading sequences for the M_k transmitted symbols on its columns. Spreading sequences are products of a base station specific scrambling sequence and channelization sequences. Orthogonal variable spreading factor (OVSF) codes are used as channelization codes. Diagonal matrix $\boldsymbol{A}_k$ contains the average received amplitudes $A_k = \sqrt{2E_b}$ for the $N_\mathrm{T}M_k$ symbols, and vector $\boldsymbol{b}_k \in \Xi_b^{N_\mathrm{T}M_k}$ (Ξ_b is symbol alphabet) contains the transmitted symbols. Noise vector contains samples from a complex zero-mean white Gaussian noise process with covariance $\sigma_n^2\mathbf{I}_{N_cN_s}$. Inter-cell interference from other base stations is modelled as a part of the white Gaussian noise.

3. RECEIVER ALGORITHMS

3.1 LMMSE Channel Equalizer

The term $\boldsymbol{DC}$ in (1) is suppressed with channel equalization. This restores the orthogonality of the channelization codes to some extent suppressing intra-cell MAI. [4]

The LMMSE equalizer is obtained from [4]

$$\boldsymbol{W}_\mathrm{L} = \arg\min_{\boldsymbol{W}} \mathrm{E}\left[\left|\boldsymbol{W}^\mathrm{H}\boldsymbol{r} - \sum_{k=1}^{\mathcal{K}} \boldsymbol{S}_k\boldsymbol{A}_k\boldsymbol{b}_k\right|^2\right], \quad (3)$$

where the minimization is carried out elementwise. By solving (3) the equalizer matrix becomes [4]

$$\boldsymbol{W}_\mathrm{L} = \left(\boldsymbol{DC}\left(\sum_{k=1}^{\mathcal{K}} \boldsymbol{A}_k^2\boldsymbol{S}_k\boldsymbol{S}_k^\mathrm{H}\right)\boldsymbol{C}^\mathrm{H}\boldsymbol{D}^\mathrm{H} + \sigma_n^2\boldsymbol{I}\right)^{-1}\boldsymbol{DC}. \quad (4)$$

The equalizer is followed by a correlator and a decision device. Thus, the decision variables for physical channel $k = 1$ are obtained from [4] $\boldsymbol{y}_\mathrm{L} = \boldsymbol{S}_1^\mathrm{H}\boldsymbol{W}_\mathrm{L}^\mathrm{H}\boldsymbol{r}$.

The presented equations are for the whole observation window. In other words, vector $\boldsymbol{y}_\mathrm{L}$ contains the decision variables for N_c/G_1 symbols. An equalizer for the nth chip is obtained from non-zero elements of the nth column from $\boldsymbol{W}_\mathrm{L}$. The block-diagram of a receiver can be seen in Fig. 1. It can be seen from (4) that the LMMSE equalizer depends on the spreading sequences of all users with the period of the long scrambling code. Thus, the optimal solution changes from chip to chip. [4]

3.2 Approximate LMMSE Channel Equalizers

3.2.1 Approximation #1

Approximation $\sum_{k=1}^{\mathcal{K}} \boldsymbol{A}_k^2\boldsymbol{S}_k\boldsymbol{S}_k^\mathrm{H} \approx s^2\sum_{k=1}^{\mathcal{K}} \boldsymbol{A}_k^2$, where s^2 denotes the square value of a chip, is made for the LMMSE equalizer presented to avoid the problem caused by the long scrambling code. After the simplification, the approximate LMMSE channel equalizer becomes [4]

$$\tilde{\boldsymbol{W}}_{\mathrm{L}1} = (s^2\sum_{k=1}^{\mathcal{K}} \boldsymbol{A}_k^2\boldsymbol{DCC}^\mathrm{H}\boldsymbol{D}^\mathrm{H} + \sigma_n^2\boldsymbol{I})^{-1}\boldsymbol{DC} \quad (5)$$

$$= \mathcal{R}_1^{-1}\boldsymbol{DC}, \quad (6)$$

where $\mathcal{R}_1$ is an approximation of the received signal covariance matrix. The decision variables after correlation becomes [4] $\boldsymbol{y}_{\tilde{\mathrm{L}}1} = \boldsymbol{S}_1^\mathrm{H}\tilde{\boldsymbol{W}}_{\mathrm{L}1}^\mathrm{H}\boldsymbol{r}$.

A single decision variable for transmit antenna n_T (i.e., an element in $\boldsymbol{y}_{\tilde{\mathrm{L}}1}$) can be written as $y_{\tilde{\mathrm{L}}1} = \boldsymbol{s}_1^\mathrm{H}\boldsymbol{z}(n)$, where $\boldsymbol{z}(n) \in \mathbb{C}^{G_1\times 1}$ is vector containing the equalizer outputs, i.e.,$(\bar{\boldsymbol{p}}_{n_\mathrm{T}})^\mathrm{H}\bar{\mathcal{R}}_1^{-1}\bar{\boldsymbol{r}}(n)$ for the desired symbol, $\bar{\boldsymbol{r}}(n) \in \mathbb{C}^{(2L+N_\mathrm{R})\times 1}$ is the part of the received signal within equalizer on the nth chip interval, $\bar{\mathcal{R}}_1$ is the part of the approximate covariance matrix corresponding to $\bar{\boldsymbol{r}}(n)$, $\bar{\boldsymbol{p}}_{n_\mathrm{T}}$ is the channel impulse response vector which corresponds to the mth symbol from transmit antenna n_T, i.e., non-zero elements in $(G_1N_\mathrm{T}m + n_\mathrm{T})$th column from the matrix $\boldsymbol{DC}$, and $\boldsymbol{s}_1$ is the spreading sequence vector for the desired physical channel.

The above approximation is reasonable as long as the received signal propagates through a common channel. However, this is not the case in MIMO communications. The above equalizer assumes that noise, intra-cell MAI and IAI deteriorate symbol estimates equally. In practice, IAI is the dominating one due to the despreading.

3.2.2 Approximation #2

The approximation #2 presented next, takes the effect of despreading into account. The order of the equalization and despreading is changed in the derivation of this new, enhanced, approximation. Thus, SINR per symbol is maximized under the assumption of a random, white scrambling sequence. The covariance matrix of the received signal after the despreading can be approximated by

$$\bar{\mathcal{R}}_2 = \bar{\mathcal{R}}_1 + (\boldsymbol{A}_1^2 - s^2\sum_{k=1}^{\mathcal{K}} \boldsymbol{A}_k^2)\sum_{n_\mathrm{T}=1}^{N_\mathrm{T}} \bar{\boldsymbol{p}}_{n_\mathrm{T}}\bar{\boldsymbol{p}}_{n_\mathrm{T}}^\mathrm{H}. \quad (7)$$

Consequently, the enhanced approximation of the LMMSE channel equalizer for transmit antenna n_T is given by

$$\tilde{\boldsymbol{w}}_{\mathrm{L}2} = \bar{\mathcal{R}}_2^{-1}\bar{\boldsymbol{p}}_{n_\mathrm{T}}. \quad (8)$$

The decision variable for the enhanced approximation becomes $y_{\tilde{\mathrm{L}}2} = \boldsymbol{s}_1^\mathrm{H}\boldsymbol{z}(n)$, where $\boldsymbol{z}(n)$ is vector containing the equalizer outputs, i.e. $\tilde{\boldsymbol{w}}_{\mathrm{L}2}^\mathrm{H}\bar{\boldsymbol{r}}(n)$ for the desired symbol. It can be easily shown that the LMMSE approximations are approaching each other, when the number of physical channels increases [8].

3.3 Spatial MAP Receiver

The spatial MAP receiver is an approximate version of the optimum multiuser detector to reduce complexity. It mitigates only IAI. The spatial MAP receiver uses the outputs from the rake receiver and the bit estimates are given by

$$\hat{\acute{\boldsymbol{b}}}_1 = \arg \max_{\acute{\boldsymbol{b}}_1 \in \{-1,1\}^{M_c N_T}} \mathcal{P}(\acute{\boldsymbol{b}}_1 | \boldsymbol{y}_R) \mathcal{P}(\acute{\boldsymbol{b}}_1), \qquad (9)$$

where $\acute{\boldsymbol{b}}_1$ is a bit vector of the desired physical channel with $M_c N_T$ elements, M_c is the size of the modulation alphabet, and maximization is carried out elementwise. The rake receiver is given by $\boldsymbol{y}_R = \boldsymbol{c}_R^H \mathcal{S}_1^H \boldsymbol{r}$, where S_1^H performs correlation of the received signal in the fingers and where $\boldsymbol{c}_R^H$ contains the complex conjugate of channel coefficients. The connection between $\acute{\boldsymbol{b}}_1$ in (9) and symbol vector $\boldsymbol{b}_1$ is $\boldsymbol{b}_1 = \Phi(\acute{\boldsymbol{b}}_1)$, where $\Phi(\cdot)$ performs mapping from bits to QPSK symbols using Gray coding.

Soft decisions are needed from the detector in order to perform efficient channel decoding. The soft decision is obtained from *a priori* and *a posteriori* log-likelihood ratios (LLR) of a transmitted bit. A priori LLR $L_a(\acute{b}_{1,k})$ is zero in the examples of this paper. A posteriori LLR of the bit $\acute{b}_{1,k}$ conditioned on the received signal $\boldsymbol{y}_R$ is given by [3]

$$L_d(\acute{b}_{1,i} \mid \boldsymbol{y}_R) = \log \frac{\mathcal{P}(\acute{b}_{1,i} = 1 | \boldsymbol{y}_R)}{\mathcal{P}(\acute{b}_{1,i} = -1 | \boldsymbol{y}_R)}, \qquad (10)$$

where $\acute{b}_{1,i}$ is ith bit from $\acute{\boldsymbol{b}}_1$ bit vector.

Encoded bits in vector $\acute{\boldsymbol{b}}_1$ can be assumed to be approximately statistically independent, due to the interleaving. Thus, a soft output value can be written as

$$L_d(\acute{b}_{1,i} \mid \boldsymbol{y}_R) = L_a(\acute{b}_{1,i}) \qquad (11)$$
$$+\log \frac{\sum_{\acute{\boldsymbol{b}}_1 \in \varphi_i^+} \exp((\boldsymbol{y}_R - \boldsymbol{c}_R^H \mathcal{S}_1^H \boldsymbol{r}_1)^H \boldsymbol{R}_n^{-1} (\boldsymbol{y}_R - \boldsymbol{c}_R^H \mathcal{S}_1^H \boldsymbol{r}_1))}{\sum_{\acute{\boldsymbol{b}}_1 \in \varphi_i^-} \exp((\boldsymbol{y}_R - \boldsymbol{c}_R^H \mathcal{S}_1^H \boldsymbol{r}_1)^H \boldsymbol{R}_n^{-1} (\boldsymbol{y}_R - \boldsymbol{c}_R^H \mathcal{S}_1^H \boldsymbol{r}_1))},$$

where $\boldsymbol{r}_1 = \boldsymbol{D}\boldsymbol{C}\boldsymbol{S}_1 \boldsymbol{A}_1 \Phi(\acute{\boldsymbol{b}}_1)$, $\boldsymbol{R}_n^{-1}$ is the covariance matrix of the noise term, φ_i^+ is the set of $2^{N_T M_c - 1}$ bit sequences $\acute{\boldsymbol{b}}_1$ having $b_{1,i} = +1$, φ_i^- is the set of $2^{N_T M_c - 1}$ bit sequences $\acute{\boldsymbol{b}}_1$ having $b_{1,i} = -1$. [3, 9]

3.4 LMMSE-MAP Receiver

LMMSE-MAP receiver is concatenation of a channel equalizer and the spatial MAP receiver. The LMMSE equalizer is used in the front part of the receiver for MAI suppression. The purpose of the spatial MAP is to suppress the residual IAI on the output of the equalizer.

When the LMMSE approximation #1 equalizer is used in the front of the spatial MAP instead of the rake receiver in (11), the soft outputs for the channel decoder is given by

$$L_d(\acute{b}_{1,i} \mid \boldsymbol{y}_R) = L_a(\acute{b}_{1,i}) \qquad (12)$$
$$+\lg \frac{\sum_{\acute{\boldsymbol{b}}_1 \in \varphi_i^+} \exp((\boldsymbol{y}_{\tilde{L}1} - \boldsymbol{p}_1^H \tilde{\mathcal{R}}_1^{-1} \boldsymbol{r}_1)^H \boldsymbol{R}_n^{-1} (\boldsymbol{y}_{\tilde{L}1} - \boldsymbol{p}_1^H \tilde{\mathcal{R}}_1^{-1} \boldsymbol{r}_1))}{\sum_{\acute{\boldsymbol{b}}_1 \in \varphi_i^-} \exp((\boldsymbol{y}_{\tilde{L}1} - \boldsymbol{p}_1^H \tilde{\mathcal{R}}_1^{-1} \boldsymbol{r}_1)^H \boldsymbol{R}_n^{-1} (\boldsymbol{y}_{\tilde{L}1} - \boldsymbol{p}_1^H \tilde{\mathcal{R}}_1^{-1} \boldsymbol{r}_1))}.$$

3.5 Complexity Discussion

There is no difference between the complexities of the two approximate equalizers. The complexity of the equalizers depends on the filter length and the update rate of filter. The complexity of filter calculation is $O(n^3)$, where n is the filter length. However, HSDPA is used with low terminal speeds, and, thus, low filter update rate can be used.

The complexity of the spatial MAP receiver increases exponentially with the N_T and M_c that makes it computationally more intensive than the approximate equalizers. The computational requirements of the spatial MAP and the LMMSE approximation #1 receivers are combined in the LMMSE-MAP receiver, that makes it computationally the most intensive from the presented receivers.

4. NUMERICAL EXAMPLES

The signal structure in the simulated system mostly follows the physical layer of the WCDMA FDD mode downlink described in [2, 7]. Adaptive modulation and coding (AMC) used in HSDPA, is not implemented. QPSK modulation is used employing root raised cosine pulses with roll-off factor of 0.22. Random cell specific scrambling code and Walsh channelization codes with spreading factor 16 are used. Two-by-two antenna MIMO transmission is used for spatial multiplexing. Signals from different antennas as well as on different physical channels are transmitted with an equal power.

The parameters of the stochastic MIMO radio channel model in 3GPP report [10] are used in the simulations. Simulations are executed in uncorrelated flat fading and ITU Vehicular A channels. The channel profiles can be found from [10]. Perfect channel state information is assumed to be known at the receiver. The known channel and receiver coefficients are used to provide the channel information needed in the turbo decoder. The variance of interference and noise needed in the decoder are estimated by averaging the squared difference of scaled transmitted signal and received signal over one TTI.

The equalizers were implemented with explicit covariance matrix inversion and equalization is performed over all the receive antennas. The equalizer length is chosen to be twice to the channel response length with components attenuated on average less than 20 dB from the peak value. The equalizer is updated at the rate of 7.5 kHz. The channel coherence time is over hundred times longer. Thus, no significant performance loss is caused due to the updating rate.

The frame error rate (FER) performance of the approximate LMMSE equalizers, spatial MAP, and LMMSE-MAP receivers is presented in uncorrelated flat fading channel in Fig. 2. SNR values for numerical examples are chosen to be E_b/N_0, where E_b is received energy per coded bit and N_0 is one sided power spectral density of noise.

The spreading sequences of the physical channels remain orthogonal in a flat fading channels. Thus, increasing the number of physical channels does not affect the perfor-

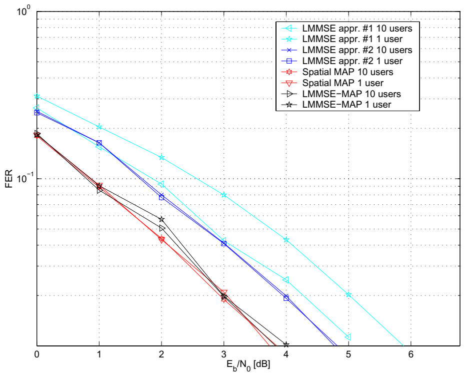

Fig. 2. FER performance in uncorrelated flat fading channel with two transmit and receive antennas.

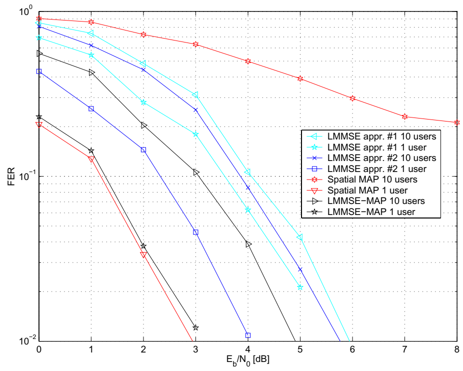

Fig. 3. FER performance in ITU Vehicular A channel with two transmit and receive antennas.

mance of the receivers. The exception is the LMMSE approximation #1 equalizer of which performance actually improves when the number of physical channels increases. The LMMSE approximation #1 equalizer does not efficiently mitigate IAI in the case of one transmitted physical channel, but it approaches the approximation #2 when the number of physical channels increases as explained in Section 3.3. The best performance is obtained with the spatial MAP and LMMSE-MAP receivers. The spatial MAP receiver can be considered as the optimal receiver in flat fading case and there is no gain achieved by using linear equalizer in front of it due to the absence of MAI.

The FER performance of the approximate LMMSE equalizers, spatial MAP, and LMMSE-MAP receivers is presented in ITU Vehicular A channel in Fig. 3. The performance of the receivers is deteriorated by both IAI and MAI due to the lost orthogonality of spreading sequences. One can note that also in this case the LMMSE approximation #1 equalizer is closer to the LMMSE approximation #2 equalizer with ten transmitted physical channels than with one transmitted physical channel. The best performance with one transmitted physical channel is given by the spatial MAP and LMMSE-MAP receivers. However, the performance of the spatial MAP receiver is significantly deteriorated by MAI with an increasing number of physical channels. The performance of LMMSE-MAP does not degrade as significantly and it gives the best performance in the case of ten transmitted physical channels.

5. CONCLUSION

Two approximate LMMSE equalizers were considered for WCDMA downlink employing MIMO communication. A receiver optimal in spatial domain was used alone and concatenated with a linear equalizer as a reference.

The results show that the receiver optimal in spatial domain does not provide performance gain enough for HSDPA connection. A good compromise, from a performance and complexity points of view, for variable traffic loads seems to be the proposed LMMSE approximation #2 receiver which suppresses both intra-cell MAI and IAI. There is no difference between the complexities of the two approximate LMMSE equalizers that makes the use of the LMMSE approximation #1 impractical due to the insufficient IAI mitigation. The concatenation of the approximate version of the optimal receiver with the LMMSE approximation #1 did not give enough performance gain over the LMMSE approximation #2 if the increase in the complexity is kept in mind.

REFERENCES

[1] G. J. Foschini and M. J. Gans, "On limits of wireless communications in a fading environment when using multiple antennas," *Wireless Personal Communications, Kluwer Academic Publishers*, vol. 6, pp. 311–335, 1998.

[2] 3rd Generation Partnership Project (3GPP); Technical Specification Group Radio Access Network, "High speed downlink packet access: Physical layer aspects (3G TS 25.858 version 5.0.0)," 3rd Generation Partnership Project (3GPP), Tech. Rep., 2002.

[3] A. Hottinen, O. Tirkkonen, and R. Wichman, Eds., *Multi-antenna Tranceiver Techiques for 3G and Beyond.* New York: John Wiley and Sons, 2003.

[4] K. Hooli, M. Juntti, M. Heikkilä, P. Komulainen, M. Latva-aho, and J. Lilleberg, "Chip-level channel equalization in WCDMA downlink," *Eurasip J. Applied Sign. Proc.*, vol. 2002, no. 8, pp. 757–770, Aug. 2002.

[5] A. Klein, "Data detection algorithms specially designed for the downlink of CDMA mobile radio systems," in *Proceedings of the IEEE Vehicular Technology Conference*, vol. 1, Phoenix, USA, May 4–7 1997, pp. 203–207.

[6] C. Berrou, A. Glavieux, and P. Thitimajshima, "Near Shannon limit error correcting coding and decoding," in *Proceedings of the IEEE International Conference on Communications*, vol. 2, Geneve, Switzerland, May 23–26 1993, pp. 1064–1070.

[7] H. Holma and A. Toskala, Eds., *Wideband CDMA for UMTS*, revised ed. New York: John Wiley and Sons, 2001.

[8] J. Ylioinas, K. Hooli, K. Kiiskila, and M. Juntti, "Interference suppression in mimo communication for WCDMA downlink," in *Proceedings of the IEEE Global Telecommunication Conference, submitted*, Dallas 29.11–3.12 2004.

[9] B. M. Hochwald and S. Brink, "Achieving near-capacity on a multiple-antenna channel," *IEEE Transactions on Communications*, vol. 51, no. 3, pp. 389–399, Mar. 2003.

[10] 3rd Generation Partnership Project (3GPP); Technical Specification Group Radio Access Network, "Spatial channel model for Multiple Input Multiple Output (MIMO) simulations (3G TR 25.996 version 6.0.0 (release 6))," 3rd Generation Partnership Project (3GPP), Tech. Rep., 2003.